Study of turbocharged diesel engine operation, pollutant emissions and combustion noise radiation during starting with bio-diesel or *n*-butanol diesel fuel blends

C.D. Rakopoulos*, A.M. Dimaratos, E.G. Giakoumis, D.C. Rakopoulos

Internal Combustion Engines Laboratory, Department of Thermal Engineering,
School of Mechanical Engineering, National Technical University of Athens,
9 Heroon Polytechniou St., Zografou Campus, 15780 Athens, Greece

ABSTRACT

The control of transient emissions from turbocharged diesel engines is an important objective for automotive manufacturers, as stringent criteria for exhaust emissions must be met. Starting, in particular, is a process of significant importance owing to its major contribution to the overall emissions during a transient test cycle. On the other hand, bio-fuels are getting impetus today as renewable substitutes for conventional fuels, especially in the transport sector. In the present work, experimental tests were conducted at the authors' laboratory on a bus/truck, turbocharged diesel engine in order to investigate the formation mechanisms of nitric oxide (NO), smoke, and combustion noise radiation during hot starting for various alternative fuel blends. To this aim, a fully instrumented test bed was set up, using ultra-fast response analyzers capable of capturing the instantaneous development of emissions as well as various other key engine and turbocharger parameters. The experimental test matrix included three different fuels, namely neat diesel fuel and two blends of diesel fuel with either bio-diesel (30% by vol.) or *n*-butanol (25% by vol.). With reference to the neat diesel fuel case during the starting event, the bio-diesel blend resulted in deterioration of both pollutant emissions as well as increased combustion instability, while the *n*-butanol (normal butanol) blend decreased significantly exhaust gas opacity but increased notably NO emission.

Keywords: Turbocharged diesel engine; Starting; Pollutant emissions; Combustion noise; Bio-diesel; *N*-butanol

* Corresponding author: Tel.: +30 210 7723529; fax: +30 210 7723531.
E-mail address: cdrakops@central.ntua.gr (C.D. Rakopoulos)

1. Introduction

So far, the study of diesel engine operation has primarily focused on its steady-state performance. However, the majority of daily driving schedules involves transient conditions, with only a very small portion of a vehicle's operating pattern being truly steady-state, e.g. when cruising on a motorway. Consequently, the investigation of diesel engine transient operation has become an important objective to automotive manufacturers, intensified by the fact of significant deviations that are experienced when comparing instantaneous transient emissions with their quasi-steady counterparts [1-7]. Recognizing the above mentioned findings, various legislative directives in the European Union, Japan and the US, have drawn the attention of manufacturers and researchers to the transient operation of (diesel) engines in the form of transient cycles certification for new vehicles [8-10].

A special, very important in terms of combustion stability and emissions, case of diesel engine transient operation is starting. Starting is distinguished as either cold or hot, depending on the respective coolant (and lube oil) temperature [11-21], with the former case being of greater importance owing to the lower temperatures involved. In vehicular applications, starting is initiated and supported by the electric starter, whereas in large unit applications (marine, industrial), the use of compressed air is favored. Only the former case is considered in the current work (vehicular engine starting), since the engine under investigation is of automotive/truck type. In such applications (and in contrary to industrial ones), hot starting is of particular importance, a fact acknowledged by various transient cycle directives [1,8,9], which include both cold and hot starting sections.

During the first cycles of a starting event, the engine accelerates rapidly with the assistance of the electric starter. Afterwards, the engine speed continues to increase without the need for external assistance, until the point where stabilization to the idling speed is achieved. An increased amount of emitted soot (primarily for turbocharged engines), unburned hydrocarbons (HC) and carbon monoxide (CO) is expected during this phase, particularly if misfiring occurs, which is more likely the colder the ambient conditions. The intriguing fact is that, unlike acceleration or load acceptance cases, during starting naturally aspirated engines suffer equally to their turbocharged counterparts [1].

As far as emissions are concerned, exhaust gases during starting have recently gained increased attention owing to their significant contribution to the total emissions from diesel-engined vehicles. For example, it has been found that a diesel engine may emit up to seven times more particulate matter during cold operation than under warm conditions [1,2], coupled also to the fact of a prolonged period of unacceptable smoke emissions [22]. The importance of (cold) starting emissions has been further documented by the legislative transient cycles, as for example the New European Driving Cycle or the US FTP-75, where the emissions are now sampled with the engine cold-started.

On the other hand, depleting crude oil reserves and growing prices have placed considerable attention on the development of alternative fuel sources [23], with particular emphasis on the bio-fuels that possess the added advantage of being renewable, showing an *ad hoc* advantage in reducing carbon dioxide (CO_2) emissions [24]. Bio-fuels made from agricultural products (oxygenated by nature) reduce the world's dependence on oil imports, support local agricultural industries, and enhance farming incomes. Moreover, they offer benefits in terms of reduced smokiness or particulate matter from diesel engines. Among those, vegetable oils or their derived bio-diesels (methyl or ethyl esters) are considered as very promising.

Experimental studies of emission measurements during steady-state and transient operation when using bio-diesel blends appear in various reported works [25-35], with all of them reporting decreases in smoke/particulate matter and moderate increases in NO emissions. Nonetheless, since most of the above (transient) investigations focus on driving cycles' operation, they provide 'mean' values for each emitted pollutant and, thus, conceal the influence and contribution of starting; this is a gap that the current work aims at filling.

Apart from bio-diesel, a very challenging (alcohol) competitor for use as fuel in compression ignition engines is ethanol and, better still, butanol [36]. Surprisingly, both have been hardly experimented with on diesel engines, let alone during starting. Butanol is of particular interest as a renewable bio-fuel as it is less hydrophilic and possesses higher heating value, higher cetane number, lower vapor pressure, and higher miscibility than ethanol; this makes it preferable to ethanol for blending with conventional diesel fuel.

The literature concerning the use of butanol/diesel fuel blends in diesel engines and its effects on their performance and exhaust emissions is very limited, a fact that constitutes another important aspect of the originality of the present work. Miers et al. [37], reported on a drive cycle analysis of *n*-butanol/diesel blends in a light-duty, turbo-diesel vehicle. Yoshimoto et al. [38] dealt with the performance and exhaust emission characteristics of diesel engine fueled with vegetable oils blended with oxygenated organic compounds, including ethanol and *n*-butanol. Armas et al. have reported results of smoke opacity during various individual transients using either vegetable oil methyl esters [39] (including starting tests) or bio-ethanol/diesel fuel blends [40]. The present research group reported recently the results during steady-state operation of two experimental investigations, viz. on a naturally aspirated, high-speed, direct injection (HSDI) diesel engine of automotive type [41], and on a turbocharged, DI, medium/heavy duty one [42]. The latter work was followed by an investigation of emissions during various acceleration schedules [43]. All these studies revealed the beneficial effects of using various blends of *n*-butanol (normal butanol) with conventional diesel fuel on the performance and exhaust emissions at various loads.

The target of the present study is to investigate the effect of diesel fuel blends with two promising bio-fuels on the transient emissions of a turbocharged diesel engine during hot starting and compare the results with the neat diesel fuel operation case, filling an apparent gap in the open literature. The two blends considered here were blends of diesel fuel with: a) 30% (by vol.) bio-diesel, and b) with 25% (by vol.) *n*-butanol; no modifications were made on the engine side when using these bio-fuels.

The experimental tests were conducted on a medium-duty, turbocharged and after-cooled, direct injection diesel engine located at the authors' laboratory, with the use of ultra-fast response emission measurement instrumentation. The experimental investigation focused on the measurement of the two most influential diesel engine pollutants, i.e. nitric oxide (NO) and smoke (in terms of opacity). Moreover, the study included also another important, but often neglected, emission, namely combustion noise. Diesel engine noise radiation is getting more and more attention in recent years [44,45], since it is associated with the passengers' and pedestrians' discomfort. The primary sources of noise generation in a diesel engine are gas flow (exhaust system), mechanical processes (e.g. valve train, gears) and combustion. Combustion noise prevails over other, mechanically originated, noise radiation [46], and this is why only this source of noise was included in the present investigation.

The instantaneous emission results are discussed in conjunction with the fuel blends composition and properties, as well as with the engine and turbocharger transient response. The differing physical and chemical properties of bio-diesel and *n*-butanol among themselves and against those of the diesel fuel are used for the analysis and interpretation of the experimental findings, shedding light into the combustion and the formation mechanisms of NO, soot, and noise, during the engine starting conditions.

2. Description of the experimental installation

A general layout of the test bed installation, the instrumentation used and the data acquisition system is illustrated in Fig. 1. A brief description of the individual components will be given in the following sub-sections. More details can be found in Ref. [19].

2.1. Engine under study

The engine used in the current study is a Mercedes-Benz OM 366 LA, turbocharged and after-cooled, direct injection diesel engine, following the Euro II emissions standard. It is widely used to power mini-buses and small/medium trucks. Its basic technical characteristics are given in Table 1. Two notable features of the engine are, on the one hand its retarded fuel injection timing in order to achieve low NO emissions and, on the other hand, the fuel-limiter (cut-off) function (pneumatic control device) in order to limit the exhaust smoke level during demanding conditions such as transients or low-speed, high-load steady-state operation.

2.2. Emissions measurement

The emissions measured in this study were the two major pollutants from diesel engines, namely nitric oxide (NO) and smoke (in terms of opacity), as well as combustion noise.

Nitric oxide (NO) was measured using the CLD500 gas analyzer by Cambustion Ltd. This is a chemiluminescent detector used for measuring NO and NO_x concentration in the exhaust gas with a 90%-10% response time of approximately 2 ms for NO and 10 ms for NO_x [47]. The non-linearity of the analyzer is less than ±1% FSO (full scale output), its drift less than ±1% FSO per hour and its accuracy is ±5 ppm. The CLD500 has two remote sampling heads and is capable of simultaneous sampling at two different locations. For the present study, only one head was applied, located downstream of the turbocharger as shown in Fig. 1. It should be mentioned at this point that it was selected to measure only NO concentration, owing to the very low values of NO_2/NO_x ratio generally encountered by diesel engines, particularly at the conditions experienced during abrupt transients. In fact, the CLD500 analyzer used was not equipped with the NO_2 to NO converter.

The exhaust gas (smoke) opacity was measured continuously with the AVL 439 partial flow opacimeter, which is particularly suitable for dynamic testing measurements with a response time less than 0.1 s and an accuracy of 0.1% opacity. The opacimeter's technical characteristics comply with legal requirements such as the ECE R24, SAE J 1667 and the ELR test cycle, with the respective filter algorithms already pre-programmed [48]. In this study, no filter algorithm was applied ('raw' signal) in order to capture successfully all the smoke emission peaks. The location of the sampling and return lines is downstream of the turbocharger (see Fig. 1).

Finally, combustion noise measurement was accomplished using the AVL 450 combustion noise meter, placed after the cylinder pressure signal amplifier (Fig. 1). Its operating principle is based on the analysis of the cylinder pressure in the frequency domain [49].

2.3. Measurement of engine and turbocharger operating parameters

The engine and turbocharger operating parameters measured and recorded continuously were: engine speed; cylinder pressure; fuel pump rack position; boost pressure and turbocharger speed. Table 2 provides a brief list of the measuring devices used. The location of each one of those on the experimental test bed installation is demonstrated in Fig. 1.

Exhaust pressures and temperatures at various locations were also measured at steady-state conditions after starting (idling) with conventional analogue devices. Additionally, fuel consumption measurements were undertaken during idling with the use of a gravimetric fuel tank. Finally, engine coolant temperature and lubricating oil pressure at idling conditions were provided through the engine instruments panel.

2.4. Data acquisition and processing system

All the above mentioned signals from the measuring devices and instruments were fed to the input of the data acquisition module, which is a Keithley KUSB 3102 ADC card connected to a Pentium Dual Core PC via USB interface. The specific card has a maximum sampling rate of 100 ksamples/s, with a 12-bit resolution for its 8 differential analogue input channels. Following the storage of the recorded measurements into files, the data were processed using an in-house developed computer code.

3. Properties of fuels tested and their blending

The conventional diesel fuel used was supplied by the Aspropyrgos Refineries of the 'Hellenic Petroleum SA' and represents the typical, Greek automotive, low sulfur (0.035% by weight) diesel fuel.

The bio-diesel used was a mixture of 50% - 50% by vol. methyl esters (ME) originating from sunflower and cottonseed oils, respectively. Blend of 30% by vol. of this was prepared by mixing with the conventional diesel fuel.

The isomer of butanol (C_4H_9OH) *n*-butanol, otherwise called 1-butanol, having a straight-chain structure and the hydroxyl group (-OH) at the terminal carbon, was used in the present study. It was of 99.9% purity (analytical grade). Butanol is a biomass-based renewable fuel that can be produced by alcoholic fermentation of the biomass feedstock (bio-butanol) [24,36]. It is very coincidental that new and innovative processes for managing and utilizing the crude glycerol co-product from the bio-diesel production processes have been developed, which convert the crude glycerol to significant yields of the value added products of mainly butanol, and 1,3-propanediol (PDO) and ethanol [50]. This is really fortunate, since the increasing demand of bio-diesel production causes serious problems with the disposal of the by-produced crude glycerol by the bio-diesel producers, given that its conversion to pure glycerol is no longer financially feasible due to the falling prices [41]. Blend of 25% by vol. of *n*-butanol was prepared by mixing with the conventional diesel fuel. Preliminary evaluation tests on the solubility of *n*-butanol in the diesel fuel with blending ratios up to 50%-50% proved that the mixing was excellent, with no phase separation for a period of several days.

It was decided to use a rather high blending ratio of both alternative bio-fuels with the conventional diesel fuel, in order for the differences to be more prominent and the underlying mechanisms better understood.

Table 3 summarizes the properties of the diesel fuel, the two methyl esters (their properties are similar) constituting the bio-diesel, and *n*-butanol. The differences in fuel properties will be used to explain qualitatively the relative emissions behavior of each fuel blend.

4. Experimental procedure

The experimental schedule included a variety of starting tests at different idling speeds and, mainly, fuel blends, all under fully warmed-up ('hot') conditions with the coolant temperature equal to 80 ºC. The detailed conditions of each test are given in Table 4. For each test, the accelerator pedal was fixed to a specific position according to the desired engine idling speed and then the starter button was initiated. Thus, the fuel pump rack was left free to shift to any position dictated by the engine speed governor, whereas the accelerator pedal was kept constant throughout each test.

Before every fuel-blend change, the engine fuel lines were cleaned and the engine was left to run for a sufficient period of time to stabilize at its new condition. Then, it was shut down with the pedal already fixed to the desired idling speed position, before initiating the starter button. Additionally, a preconditioning procedure was followed between each fuel change in order to remove the deposited particulate matter on the exhaust pipe walls, which could be blown out and released during the following starting tests [51], thus leading to 'faulty' measurements of smoke opacity and erroneous interpretations for each fuel blend and its effects on smoke emission.

5. Results and discussion

5.1. Engine starting tests using neat diesel fuel at various idling speeds – Tests No. 1 & 2

The first two tests were performed using neat diesel fuel, at two different idling speeds (see also Table 4); these tests were used as the baseline for the bio-fuels trials that followed. The accelerator pedal was set to the desired idling speed position, the engine was shut down and it was started immediately via initiation of the starter button. Consequently, there was no time for the engine to cool down and for the fuel pump rack to return to its minimum position. The development of five engine and turbocharger operating parameters is illustrated in Fig. 2 (engine speed, fuel pump rack position, peak cylinder pressure, turbocharger speed, and boost pressure).

For both cases in Fig. 2, the fuel pump rack initiates exactly from the position reached during the preceding shut-downs, gradually shifting backwards as the engine attains the governing self-sustained speed. This would not be the case, however, for cold starting, where the fuel pump rack would initiate from its minimum position. The higher the idling speed, as in test No. 1, the longer the time the rack remains in the maximum fueling position, before stabilizing to its (higher) final steady-state point. One should notice the initial sharp speed increase (lower-left sub-diagram of Fig. 2) that derives as a result of the electric starter action; as expected, after the disengagement of the starter (at the 3rd cycle or after 1.5 sec), the engine accelerates at a slower rate.

During the early seconds of the transient event, there was a relative lack of air-flow due to the low engine and turbocharger rotational speeds. Recall that for aerodynamic type compressors, such as the ones used in turbochargers, boost pressure and air-flow are strongly dependent on turbocharger speed. Consequently, locally high fuel-air ratios were experienced, leading to flame quenching (owing to oxygen shortage) and combustion instability; the latter is further documented in the variability of peak pressures (upper-left sub-diagram of Fig. 2). As the engine speed gradually increased, the rack moved progressively to a lower fuel supply until it ultimately assumed its final steady-state position after the engine had reached its idling, self-sustained speed.

The thermal condition of the engine and the required idling speed were the two major contributors responsible for the turbocharger response too; compared with a cold starting event, however, the latter accelerated faster, owing to the much higher exhaust gas energy content, originating in the (much) lower heat loss to the now fully warmed-up cylinder and exhaust manifold walls. Finally, and following engineering intuition, both the turbocharger speed and the compressor boost pressure assume higher values for the case of higher engine idling speed (test No. 1) compared with the lower idling speed of test case No. 2.

Another interesting finding concerns the combustion behavior during idling. After the engine speed has stabilized, combustion appears to be much more stable during test No. 1; this is documented by the almost constant maximum cylinder pressure traces illustrated in the upper sub-diagram of Fig. 2. Closer examination of the cylinder pressure traces between the 55th and the 80th engine cycle is further provided in Fig. 3, supporting this observation. There is evident combustion instability during test No. 2; however, no misfire was observed, most probably owing to the already warmed-up conditions. The different engine idling speed between tests No. 1 and 2 is the obvious reason for that behavior [11]. The higher idling speed of test No. 1 produces higher compression pressures and temperatures ensuring faster ignition, while the higher air-supply promotes combustion [1].

Moreover, the higher injection pressures encountered during test No. 1 (owing to the higher engine speed [52]) combined with the higher in-cylinder turbulence levels favor fuel-air mixing, promoting in this way faster ignition. On the other hand, the lower idling engine speed of test No. 2 causes higher blow-by loss past the piston rings compared with the previous case and allows more time for the heat loss to develop [1]. Thus, lower compression pressures (and temperatures) are developed [53], worsening the combustion process and resulting eventually in the combustion instability observed in the lower sub-diagram of Fig. 3.

Unsurprisingly, the previously mentioned phenomena have also a direct impact on the pollutant emissions and combustion noise radiation, as illustrated in Fig. 4. The exhaust gas opacity instantaneously assumes very high values during both tests of the order of 60% (lower-right sub-diagram of Fig. 4). The peak opacity values are attributed to turbocharger lag, being prominent mainly during the early cycles. It is reminded that net soot production is mainly dependent on the fuel-air equivalence ratio (i.e. the actual fuel-air ratio divided by its stoichiometric value). During the turbocharger lag cycles, a mismatch exists between the injected fuel quantity (quite large as implied by the fuel pump rack position sub-diagram in Fig. 2) and the still small air-supply owing to the inertia of the turbocharger; thus, the fuel-air equivalence ratio increases beyond the stoichiometric value (of 1.0) and the production of soot is favored.

The higher engine idling speed (test No. 1) induces also higher peak opacity values and prolonged smoky period. During test No. 1, smoke opacity exceeds 10% for 17 engine cycles (2.9 sec), while in test No. 2 this happens for ‘only’ 9 cycles (1.5 sec). The reason for this behavior is that for the higher idling speed (test No. 1), a larger discrepancy exists between the fuel pump rack displacement with the relatively limited air-supply following turbocharger lag during the early cycles.

As far as NO emission is concerned (lower-left sub-diagram of Fig. 4), in general, similar values are experienced for both tests, i.e. No. 1 and 2. The higher final values of NO observed during test No. 1 compared with the ones of test No. 2 are attributed, as discussed previously, to the greater fuel pump rack displacements and the higher combustion pressures. In order to analyze the NO trend, the contribution of various parameters has to be taken into account. On the one hand, the low boost pressures, resulting in low oxygen availability, do not favor NO formation inside the cylinder. On the other hand, the increase of the ignition delay period combined with injection timing alteration (due to the very low engine speed), and the increased values of fuel-air equivalence ratio, locally reaching stoichiometry, are well known to promote NO production.

Moreover, for the NO results illustrated in Fig. 4, an important factor determining their values is the units used for the quantification of NO. The volumetric concentration (ppm) assumes higher values the lower the engine rotational speed and may thus lead to erroneous interpretations [54], because air mass is not suitably integrated with the 'ppm' values. Furthermore, during starting, the air-supply is initially small due to the low boost pressure and turbocharger speed, resulting in high concentration values, when the mass of NO is reduced to the total exhaust gas mass as is the case in the present study.

The last class of emission studied is combustion noise, which is notably affected by two factors, i.e. the required idling speed and the cylinder pressure development (upper sub-diagram of Fig. 4). In fact, its measuring principle is based on the processing of the measured indicator diagrams. Combustion noise (or otherwise stated, combustion roughness) is determined by the cylinder pressure rise rate (i.e. its gradient with respect to crank angle) during the engine cycle [46]. This rate is influenced by a variety of parameters, including injection timing and ignition delay. Under cold starting conditions, both these parameters behave significantly differently compared with the fully warmed-up, steady-state engine operation. Particularly, the ignition delay effect is most influential; the lower temperatures in the combustion chamber prevent fast fuel ignition, leading to a prolonged premixed combustion phase, hence steeper cylinder pressure gradients and, consequently, higher combustion noise levels. Things run quite smoother during the hot starting events studied here, however, since the engine thermal status practically corresponds to fully warmed-up conditions. The only serious discrepancy arises again from the turbocharger lag phenomenon. The latter may induce locally very high fuel-air equivalence ratios and prohibit timely ignition. All in all, it is observed that the ignition delay is not much aggravated and, consequently, no significant increase in the duration of premixed combustion and in the pressure gradient is experienced.

Nonetheless, the second contributing factor, namely the required idling speed seems to play an important role here; during the higher idling speed test No. 1, combustion noise assumes higher values, due to the steeper cylinder pressure increase required to reach the higher self-sustained speed.

5.2. *Engine starting tests using blends of diesel fuel with bio-diesel (Test No. 3) or n-butanol (Test No. 4)*

The experimental study was extended with the investigation of the hot starting event of test No. 2 (idling speed 950 rpm), but with the engine running now on blends of diesel fuel with bio-diesel or *n*-butanol. For test No. 3, the blend used consisted of 70% diesel fuel and 30% bio-diesel (by vol.), while for test No. 4 it was 75% diesel fuel and 25% *n*-butanol (by vol.). Details about each blend and the properties of each constituent were provided in Table 3. The development of five engine and turbocharger operating parameters for the test cases examined is illustrated in Fig. 5, together with the neat diesel fuel results, in order for the trends and absolute values to be directly comparable.

As with the case of the engine running on neat diesel fuel, the fuel pump rack in Fig. 5 lies initially at its maximum position reached during the preceding engine shut-down. After initiation of the starting, the rack gradually shifts to a final (lower) position corresponding to the required idling speed, as determined by the (accelerator) pedal setting. The differentiations observed in the rack profile development are small for all fuels tested, and these are also reflected into minor deviations in engine speed development and turbocharger response. A first finding, therefore, is that the bio-fuel blend does not seem to affect the engine and turbocharger starting response and performance, at least for blends up to 30% by vol. of bio-diesel or *n*-butanol. This was also the result reached during a similar experimental investigation for acceleration transients [43]. As with all the test cases examined, independently of the fuel blend used, the initial sharp increase in engine speed is due to the electric starter action.

A further notable finding concerns the development of combustion. A closer examination of the cylinder pressure diagrams during the first 25 cycles of the hot starting events for each fuel blend is provided in Fig. 6. It is revealed that a higher degree of combustion instability is experienced by the bio-diesel blend, whereas its *n*-butanol counterpart seems more stable (as it is also the case with the neat diesel fuel operation) despite its lower cetane number. This is also documented in the lower sub-diagram of Fig. 7. In the same figure it is also revealed that during the bio-diesel blend hot starting, the engine experiences higher cycle-by-cycle peak cylinder pressure variability; the latter is further quantified in

Table 5 (mean value and standard deviation of the maximum cylinder pressure during the first 25 cycles of tests No. 2, 3 and 4) for comparative purposes.

Clearly, the high value of the deviation for the bio-diesel blend in Table 5 indicates more intense combustion instability. On the other hand, a major reason for the higher pressures experienced for the *n*-butanol blend (indicated by its higher mean value) is its lower cetane number, which leads to longer ignition delay. However, misfire was not an issue for either bio-fuel blend used, probably owed to the already warmed-up engine conditions. The above-mentioned behavior can be attributed to the different injection and combustion process of each fuel blend. It is reminded that the whole fuel system of the engine is optimized for neat diesel fuel operation. The dissimilar physical and chemical properties of each constituent of the blends result in alteration of the fuel delivery, dynamic injection timing [55], fuel spray dispersion, wall impingement rate, ignition delay, as well as fuel evaporation and mixing rates [56]. As a result, the premixed and diffusion parts of combustion vary, while the presence of oxygen in the bio-fuel blends is responsible for different local fuel-air equivalence ratios, favoring or preventing the initiation of combustion.

It is the development of the pollutant emissions that present significant differences when comparing the results of the two bio-fuel blends against those of the neat diesel fuel operation (lower sub-diagrams of Fig. 8). However, the effect of each bio-fuel on the smoke emissions is contradicting, viz. the bio-diesel blend increases both the peak soot value and the unacceptable smoky period, whereas its *n*-butanol counterpart substantially decreases both of them, compared with the neat diesel fuel case (relative differences of the order of +40% and -69%, respectively, in the maximum opacity value). Moreover, opacity exceeds the 10% value for 10, 14 and just 3 engine cycles (or 1.9, 2.5 and 0.5 sec), respectively, for the neat diesel fuel, the bio-diesel and the *n*-butanol blends cases.

Although the oxygen content in the bio-diesel has been identified as the main contributor for lower smoke emissions during steady-state and transient operation under fully warmed-up conditions, it is its higher viscosity that plays the most decisive role during starting. Consequently, the rate of spray atomization is reduced [1] and greater mixture heterogeneity is experienced, leading to the increased smoke emissions demonstrated in the lower-right sub-diagram of Fig. 8 and also to the extended pressure variability (Figs. 6 and 7) discussed earlier. This finding confirms the results of Armas et al. [39], who measured up to 80% higher absolute opacity values on a HSDI engine during cold starting running on neat bio-diesel. In the cold starting case, however, it is also the higher initial boiling point of bio-diesel with respect to conventional diesel fuel, which leads to more difficult fuel evaporation at low ambient temperatures and further worsening of the fuel–air mixing mechanism.

On the other hand, for the diesel-butanol blend, the improvement in smoke emissions should be attributed to the engine running overall ‘leaner’, since combustion is now assisted by the presence of the (now higher) fuel-bound oxygen of the butanol in the locally rich zones, which seems to have the dominant influence; this was also the result reached by Miyamoto et al. [57]. Similar promising results, when using diesel-butanol blends, have been reported recently by the present research group during steady-state operations of a naturally aspirated HSDI and a turbocharged DI diesel engine [41,42], with these studies showing that the degree of smoke emission improvement was better the higher the percentage of *n*-butanol in its blend with the diesel fuel.

One might argue, at this point, that the extra oxygen in the fuel is very small with respect to its value in the air to provoke leaning of the mixture. This may be true during turbocharged diesel engine steady-state operation or during steady-state or transient operation of naturally aspirated engines. However, one should not forget that during transients of turbocharged diesel engines, this extra oxygen is available inside the cylinder at the point and time where a significant deficiency of air exists from the compressor (turbocharger lag). And so, indeed, it proves extremely crucial for the combustion mechanism and the emission formation described herein.

As regards NO emission (in ppm), this peaks during starting for both bio-fuel blends at higher values compared with the neat diesel fuel (lower-left sub-diagram of Fig. 8), and this trend is actually maintained throughout the stabilization, steady-state phase. Concerning the absolute peak values, the bio-diesel blend increased NO by 30% and the *n*-butanol blend by 51%. The combination of the two major parameters determining NO formation, namely combustion temperature and oxygen availability, should be accounted for in order to interpret these results [58,59]. It is likely that lower (global) temperatures may exist for the bio-diesel and the *n*-butanol cases, as the engine runs overall ‘leaner’ (owing to the fuel-bound oxygen, which is much higher for *n*-butanol than for the bio-diesel, Table 3). In the case of bio-diesel, this lower temperature may also be attributed to its lower calorific value. By the same token, in the case of *n*-butanol, this lower temperature may be attributed to both its lower calorific value and its higher heat of evaporation. However, the latter can be offset by the opposing effect of the lower cetane number (and thus longer ignition delay) of the *n*-butanol (see also Table 3), leading possibly to higher local temperatures during the premixed part of combustion where NO is predominantly formed.

The higher NO values, however, with respect to the neat diesel fuel case, suggest that the local oxygen availability has the dominant effect. The higher values of the fuel-bound oxygen for the bio-diesel and the *n*-butanol blends against the neat diesel fuel may be bringing locally the ‘prepared’ mixture nearer to stoichiometry (towards the lean) during the premixed combustion phase (when NO is mainly formed), thus leading to the relative increase of NO formation. In any case, the leanness and the combustion temperature of the mixture on a local basis form a delicate balance on NO formation, weighting more or less on the one or the other side, depending on the type of blends, and the specific engine calibration and operating conditions.

Concerning the third emission considered in this investigation, i.e. combustion noise, minimal deviations are observed between the three cases examined, as demonstrated in the upper sub-diagram of Fig. 8. Although the injection and the combustion process vary from one blend to the other, as detailed above, it seems that the noise radiation is not practically affected by the fuel blend used. This is particularly important for the *n*-butanol blend. Butanol has a low cetane number compared with the conventional diesel or bio-diesel (Table 3). Then, one would expect longer ignition delay period, hence steeper pressure gradients and so higher noise radiation. However, it seems that during the rough conditions of starting it is: a) the inherent combustion instability and cylinder pressure variation from cycle to cycle, and b) the low cranking speed, that have the dominant effect on the noise radiation. In particular, the low cranking speed induces low cylinder pressure increase rates *overall* during starting, irrespective of the fuel blend used.

6. Summary and conclusions

A fully instrumented test bed installation has been set up in order to study the transient performance and emissions of a bus/truck turbocharged diesel engine during hot starting. Ultra-fast response analyzers were employed for measuring nitric oxide, smoke opacity and combustion noise emissions. A variety of starting tests was conducted for different fuel blends, i.e., neat diesel fuel or diesel fuel with either bio-diesel or *n*-butanol, with blending ratios of 70%-30% and 75%-25% (by vol.), respectively. The composition and physical and chemical properties of each fuel blend were used for the analysis and interpretation of the experimental findings. As a general remark, unlike cold starting tests, the thermal status of the engine (fully warmed-up conditions) limited the discrepancies compared with steady-state operation.

The basic conclusions derived from the current investigation, for the specific engine-brake configuration and fuel blends tested, are summarized below:

- As expected, turbocharger lag was found to be the most notable contributor for all starting discrepancies and the major cause of peak pollutant emission values for every fuel blend used.
- The low cranking speed appeared to have the dominant influence on combustion noise development and its absolute values.
- Combustion behavior and stability during the first transient cycles were affected mostly by the bio-diesel blend and less by the *n*-butanol blend. Moreover, combustion appeared to be more stable at higher idling speeds.
- Smoke opacity increased notably (+40% in peak value) for the bio-diesel blend, while for the *n*-butanol blend it decreased significantly (-69% in peak value).
- For both bio-fuel blends, NO emission increased compared with the neat diesel fuel case; specifically, peak NO value increased by 30% and 51% for the bio-diesel and *n*-butanol blends, respectively.
- The biofuels blends had a minor effect on the transient performance of the engine (engine speed development, turbocharger response) and the overall combustion noise radiation.

Acknowledgements

The authors would like to thank Cambustion Ltd. (Cambridge, U.K.) for the loan of the CLD500 NO analyzer and, particularly, Dr. M.S. Peckham for his support during the experimental investigation of the engine. Special thanks are due to Turbo Hellas Trading Ltd. for the donation of the turbocharger speed sensor kit used in the experiments.

References

[1] Rakopoulos CD, Giakoumis EG. Diesel engine transient operation. London: Springer; 2009.

[2] Bielaczyc P, Merkisz J, Pielecha J. Investigation of exhaust emissions from DI diesel engine during cold and warm start. SAE Paper no. 2001-01-1260; 2001.

[3] Rakopoulos CD, Giakoumis EG. Review of thermodynamic diesel engine simulations under transient operating conditions. SAE Paper no. 2006-01-0884; 2006.

[4] Hagena JR, Filipi ZS, Assanis DN. Transient diesel emissions: analysis of engine operation during a tip-in. SAE Paper no. 2006-01-1151; 2006.

[5] Wijetunge RS, Brace CJ, Hawley JG, Vaughan ND, Horrocks RW, Bird GL. Dynamic behaviour of a high speed direct injection diesel engine. SAE Paper no. 1999-01-0829; 1999.

[6] Black J, Eastwood PG, Tufail K, Winstanley T, Hardalupas Y, Taylor AMKP. Diesel engine transient control and emissions response during a European extra-urban drive cycle (EUDC). SAE Paper no. 2007-01-1938; 2007.

[7] Eastwood PG, Tufail K, Winstanley T, Darlington A, Karagiorgis S, Hardalupas Y, Taylor AMKP. Estimation of deviations in NO and soot emissions between steady-state and EUDC transient operation of a common-rail diesel engine. SAE Paper no. 2009-24-0147; 2009.

[8] U.S. Environmental Protection Agency (EPA), Testing and Measuring Emissions, Engine Brake Dynamometer Duty Cycles, http://www.epa.gov/nvfel/testing/dynamometer.htm#engcycles, 2009 [accessed 15.09.10].

[9] European Commission, Enterprise and Industry, Automotive section: Directives and Regulations on Motor Vehicles, http://ec.europa.eu/enterprise/sectors/automotive/documents/directives/motor-vehicles/, 2009 [accessed 15.09.10].

[10] Giakoumis EG, Alafouzos AI. Study of diesel engine performance and emissions during a Transient Cycle applying an engine mapping-based methodology. Appl Energy 2010;87:1358-65.

[11] Henein NA, Zahdeh AR, Yassine MK, Bryzik W. Diesel engine cold starting: combustion instability. SAE Paper no. 920005; 1992.

[12] Belardini P, Bertoli C, Del Giacomo N, Iorio B. Combustion and pollutant emissions from light duty diesel engines: the influence of mixing process and transient operating conditions. Sci Total Environ 1993;134(1-3):285-93.

[13] Osuka I, Nishimura M, Tanaka Y, Miyaki M. Benefits of new fuel injection technology on cold startability of diesel engines – improvement of cold startability and white smoke reduction by means of multi injection with common rail fuel system (ECD-U2). SAE Paper no. 940586; 1994.

[14] Ogawa H, Raihan KA, Ilizuka K-I, Miyamoto N. Cycle-to-cycle transient characteristics of diesel emissions during starting. SAE Paper no. 1999-01-3495; 1999.

[15] Bielaczyc P, Merkisz J, Pielecha J. Exhaust emissions from diesel engine during cold start in ambient temperature conditions. SAE Paper no. 2000-05-0316; 2000.

[16] Cotte H, Bessagnet B, Blondeau C, Mallet-Hubert P-Y, Momique J-C, Walter C, Boulanger L, Deléger D, Jouvenot G, Clarisse P, Rouveirolles P. Cold-start emissions from petrol and diesel vehicles according to the emissions regulations (from euro 92 to euro 2000). Int J Veh Des 2001;27(1-4):275-85.

[17] Engler D, Hausberger S, Blassnegger J. Cold start emissions of heavy duty vehicles. SAE Paper no. 2001-24-0077; 2001.

[18] Weilenmann M, Soltic P, Saxer C, Forss A-M, Heeb N. Regulated and nonregulated diesel and gasoline cold start emissions at different temperatures. Atmos Environ 2005;39(13):2433-41.

[19] Rakopoulos CD, Dimaratos AM, Giakoumis EG, Peckham MS. Experimental assessment of turbocharged diesel engine transient emissions during acceleration, load change and starting. SAE Paper no. 2010-01-1287; 2010.

[20] Peng H-Y, Cui Y, Deng K-Y, Shi L, Li L-G. Combustion and emissions of a direct-injection diesel engine during cold start under different exhaust valve closing timing conditions. Proc IMechE, Part D: J Automobile Eng 2008;222(1):119-29.

[21] Khalek IA, Ullman TL, Vasquez L, Guerrero M. Hot start transient emissions from a Mercedes OM 366 LA and a Detroit Diesel Operated on Chilean, California, and US 2D Fuels. SAE Paper no. 2002-01-2827; 2002.

[22] Arcoumanis C, Yao XG. Transient smoke and unburnt hydrocarbon emissions during cold-start in a turbo-charged DI diesel engine. IMechE Seminar on "Transient Performance of Engines" 1994:43-60.

[23] Lin L, Cunshan Z, Vittayapadung S, Xiangqian S, Mingdong D. Opportunities and challenges for biodiesel fuel. Appl Energy 2011;88:1020-31.

[24] Hansen AC, Kyritsis DC, Lee CF. Characteristics of biofuels and renewable fuel standards, In: Vertes AA et al. editors. Biomass to biofuels - strategies for global industries. New York: John Wiley; 2009.

[25] Graboski MS, Ross JD, McCormick RL. Transient emissions from No. 2 diesel and biodiesel blends in a DDC series 60 engine. SAE Paper no. 961166; 1996.

[26] Starr ME. Influence on transient emissions at various injection timings, using cetane improvers, bio-diesel, and low aromatic fuels. SAE Paper no. 972904; 1997.

[27] Agarwal AK, Rajamanoharan K. Experimental investigations of performance and emissions of Karanja oil and its blends in a single cylinder agricultural diesel engine. Appl Energy 2009;86:106-12.

[28] Sharp CA, Howell SA, Jobe J. The effect of biodiesel fuels on transient emissions from modern diesel engines - part I: regulated emissions and performance. SAE Paper no. 2000-01-1967; 2000.

[29] Qi DH, Chen H, Geng LM, Bian YZ, Ren XC. Performance and combustion characteristics of biodiesel-diesel-methanol blend fuelled engine. Appl Energy 2010;87:1679-86.

[30] Wang WG, Lyons DW, Clark NN, Gautam M, Norton PM. Emissions from nine heavy trucks fueled by diesel and biodiesel blend without engine modification. Environ Sci Technol 2000;34(6):933-9.

[31] Durbin TD, Cocker DR III, Sawant AA, Johnson K, Miller JW, Holden BB, Helgeson NL, Jack JA. Regulated emissions from biodiesel fuels from on/off road applications. Atmos Environ 2007;41(27):5647-58.

[32] Fontaras G, Karavalakis G, Kousoulidou M, Tzamkiozis T, Ntziachristos L, Bakeas E, Stournas S, Samaras Z. Effects of biodiesel on passenger car fuel consumption, regulated and non-regulated pollutant emissions over legislated and real-world driving cycles. Fuel 2009;88(9):1608-17.

[33] Devan PK, Mahalakshmi NV. A study of the performance, emission and combustion characteristics of a compression ignition engine using methyl ester of paradise oil-eucalyptus oil blends. Appl Energy 2009;86:675-80.

[34] Lujan JM, Bermudez V, Tormos B, Pla B. Comparative analysis of a DI diesel engine fuelled with biodiesel blends during the european MVEG-A cycle: performance and emissions (II). Biomass Bioenergy 2009;33(6-7):948-56.

[35] Hazar H, Aydin H. Performance and emission evaluation of a CI engine fueled with preheated raw rapeseed oil (RPO)-diesel blends. Appl Energy 2010;87(3):786-90.

[36] Kumar M, Gayen K. Developments in biobutanol production: New insights. Appl Energy 2011;88:1999-2012.

[37] Miers SA, Carlson RW, McConnell SS, Ng HK, Wallner T, Esper JL. Drive cycle analysis of butanol/diesel blends in a light-duty vehicle. SAE Paper no. 2008-01-2381; 2008.

[38] Yoshimoto Y, Onodera M. Performance of a diesel engine fueled by rapeseed oil blended with oxygenated organic compounds. SAE Paper no. 2002-01-2854; 2002.

[39] Armas O, Hernandez JJ, Cardenas MD. Reduction of diesel smoke opacity from vegetable oil methyl ester during transient operation. Fuel 2006;85(17-18):2427-38.

[40] Armas O, Cardenas MD, Mata C. Smoke opacity and NO_x emissions from a bioethanol-diesel blend during engine transient operation. SAE Paper no. 2007-24-0131; 2007.

[41] Rakopoulos DC, Rakopoulos CD, Giakoumis EG, Dimaratos AM, Kyritsis DC. Effects of butanol-diesel fuel blends on the performance and emissions of a high-speed DI diesel engine. Energy Convers Manage 2010;51(10):1989-97.

[42] Rakopoulos DC, Rakopoulos CD, Hountalas DT, Kakaras EC, Giakoumis EG, Papagiannakis RG. Investigation of the performance and emissions of a bus engine operating on butanol/diesel fuel blends. Fuel 2010;89(10):2781-90.

[43] Rakopoulos CD, Dimaratos AM, Giakoumis EG, Rakopoulos DC. Investigating the emissions during acceleration of a turbocharged diesel engine operating with bio-diesel or n-butanol diesel fuel blends. Energy 2010;35(12):5173-84.

[44] Commission Directive 96/20/EC of 27 March 1996. Adapting to technical progress council directive 70/15/EEC relating to the permissible sound level and the exhaust system of motor vehicles, Official journal L 092, April 1996.

[45] Dhaenens M, Van der Linden G, Nehl J, Thiele R. Analysis of transient noise behaviour of a truck diesel engine. SAE Paper no. 2001-01-1566; 2001.

[46] Lilly LRC. Diesel Engine Reference Book. London: Butterworths; 1984.

[47] CLD500 Fast NO_x Measurement System. User Manual (version 2.2). Cambustion Ltd. 2008.

[48] AVL 439 Opacimeter. Operating Manual. AVL 2006.

[49] AVL 450 Combustion Noise Meter. Operating Manual. AVL 2000.

[50] Taconi KA, Venkataramanan KP, Johnson DT. Growth and solvent production by clostridium pasteurianum (ATCC, 6013) utilizing biodiesel-derived crude glycerol as the sole carbon source. AIChE, Environ Prog Sustain Energy 2009;28(1):100-10.

[51] Andrews GE, Clarke AG, Rojas NY, Sale T, Gregory D. The transient storage and blow-out of diesel particulate in practical exhaust systems. SAE Paper no. 2001-01-0204; 2001.

[52] Heywood JB. Internal combustion engine fundamentals. New York: McGraw-Hill; 1988.

[53] Cheng KY, Shayler PJ, Murphy M. The influence of blow-by on indicated work output from a diesel engine under cold start conditions. Proc IMechE, Part D: J. Automobile Engineering 2004;218:333-40.

[54] Grados CVD, Uriondo Z, Clemente M, Espadafor FJJ, Gutiérrez JM. Correcting injection pressure maladjustments to reduce NO_x emissions by marine diesel engines. Transp Res, Part D: Transp Environ 2009;14(1):61-6.

[55] Ban-Weiss GA, Chen JY, Buchholz BA, Dibble RW. A numerical investigation into the anomalous slight NO_x increase when burning biodiesel; a new (old) theory. Fuel Proc Technol 2007;88(7):659-67.

[56] Rakopoulos CD, Antonopoulos KA, Rakopoulos DC. Multi-zone modeling of diesel engine fuel spray development with vegetable oil, bio-diesel or diesel fuels. Energy Convers Manage 2006;47(11-12):1550-73.

[57] Miyamoto N, Ogawa H, Nabi MN. Approaches to extremely low emissions and efficient diesel combustion with oxygenated fuels. Int J Engine Res 2000;1(1):71-85.

[58] Rakopoulos CD, Antonopoulos KA, Rakopoulos DC. Development and application of a multi-zone model for combustion and pollutants formation in a direct injection

diesel engine running with vegetable oil or its bio-diesel. Energy Convers Manage 2007;48(7):1881-901.

[59] Rakopoulos CD, Rakopoulos DC, Giakoumis EG, Kyritsis DC. The combustion of n-butanol/diesel fuel blends and its cyclic variability in a DI diesel engine. Proc IMechE, Part A: J Power Energy 2010 (accepted for publication).

Figures Captions

Fig. 1 Schematic arrangement of the test bed installation, instrumentation and data acquisition system.

Fig. 2 Development of engine and turbocharger response during hot starting at two idling speeds, for the neat diesel fuel operation (tests No. 1 & 2).

Fig. 3 Cylinder pressure diagrams during idling, for the neat diesel fuel operation (tests No. 1 & 2).

Fig. 4 Development of exhaust emissions and noise radiation during hot starting at two idling speeds, for the neat diesel fuel operation (tests No. 1 & 2).

Fig. 5 Development of engine and turbocharger response during hot starting, with varying fuel blends (tests No. 2, 3 and 4).

Fig. 6 Cylinder pressure diagrams during the first 25 cycles of hot starting, with varying fuel blends (tests No. 2, 3 and 4).

Fig. 7 Maximum cylinder pressure and its cycle-by-cycle variability during the first 25 cycles of hot starting, with varying fuel blends (tests No. 2, 3 and 4).

Fig. 8 Development of exhaust emissions and noise radiation during hot starting, with varying fuel blends (tests No. 2, 3 and 4).

Tables Captions

Table 1 Engine and turbocharger specifications.

Table 2 Measuring devices for the engine and turbocharger operating parameters.

Table 3 Properties of diesel fuel, methyl esters (ME) of sunflower and cottonseed oils, and *n*-butanol.

Table 4 Tabulation of test conditions.

Table 5 Mean value and standard deviation of the maximum cylinder pressure during the first 25 cycles of hot starting, with varying fuel blends (tests No. 2, 3 and 4).

Table 1

Engine model and type	‘Mercedes Benz’, OM 366 LA, 6 cylinder, in-line, 4-stroke, compression ignition, direct injection, water-cooled, turbocharged, after-cooled, with bowl-in-piston
Emissions standard	Euro II
Speed range	800–2600 rpm
Maximum power	177 kW @ 2600 rpm
Maximum torque	840 Nm @ 1250–1500 rpm
Engine total displacement	5958 cm^3
Bore/Stroke	97.5 mm / 133 mm
Compression ratio	18:1
Fuel pump	‘Bosch’ PE-S series, in-line, 6-cylinder with fuel limiter
Static injection timing	5±1 degrees crank angle before TDC (at full load)
Turbocharger model	‘Garrett’ TBP 418-1 with internal waste-gate

Table 2

Parameter	Measuring device
Engine speed	‘Kistler’ shaft encoder
Cylinder pressure	‘Kistler’ miniature piezoelectric transducer, combined with ‘Kistler’ charge amplifier
Fuel pump rack position	Linear Variable Differential Transducer (LVDT)
Boost pressure	‘Wika’ pressure transmitter
Turbocharger speed	‘Garrett’ turbo-speed sensor (including gauge)

Table 3

Fuel properties	Diesel fuel	Sunflower ME	Cottonseed ME	*N*-Butanol
Density at 20ºC, kg/m^3	837	880	885	810
Cetane number	50	50	52	~25
Lower calorific value, MJ/kg	43	37.5	37.5	33.1
Kinematic viscosity at 40ºC, mm^2/s	2.6	4.4	4	3.6^+
Boiling point ºC	180-360	345	345	118
Latent heat of evaporation, kJ/kg	250	230	230	585
Oxygen, % weight	0	10.9	10.9	21.6
Stoichiometric air-fuel ratio	15.0	12.5	12.5	11.2
Molecular weight	170	284	284	74

$^+$Measured at 20ºC

Table 4

Test No.	Fuel blend	Idling speed (rpm)	Lubricating oil pressure (bar)
1	100% diesel	1215	2.5
2	100% diesel	950	1.8
3	70% diesel - 30% bio-diesel	950	1.8
4	75% diesel - 25% *n*-butanol	950	1.8

Table 5

Fuel blend	Mean value (bar)	Standard deviation (bar)
100% diesel	77.3	6.8
70% diesel - 30% bio-diesel	74.6	10.2
75% diesel - 25% *n*-butanol	81.5	8.2

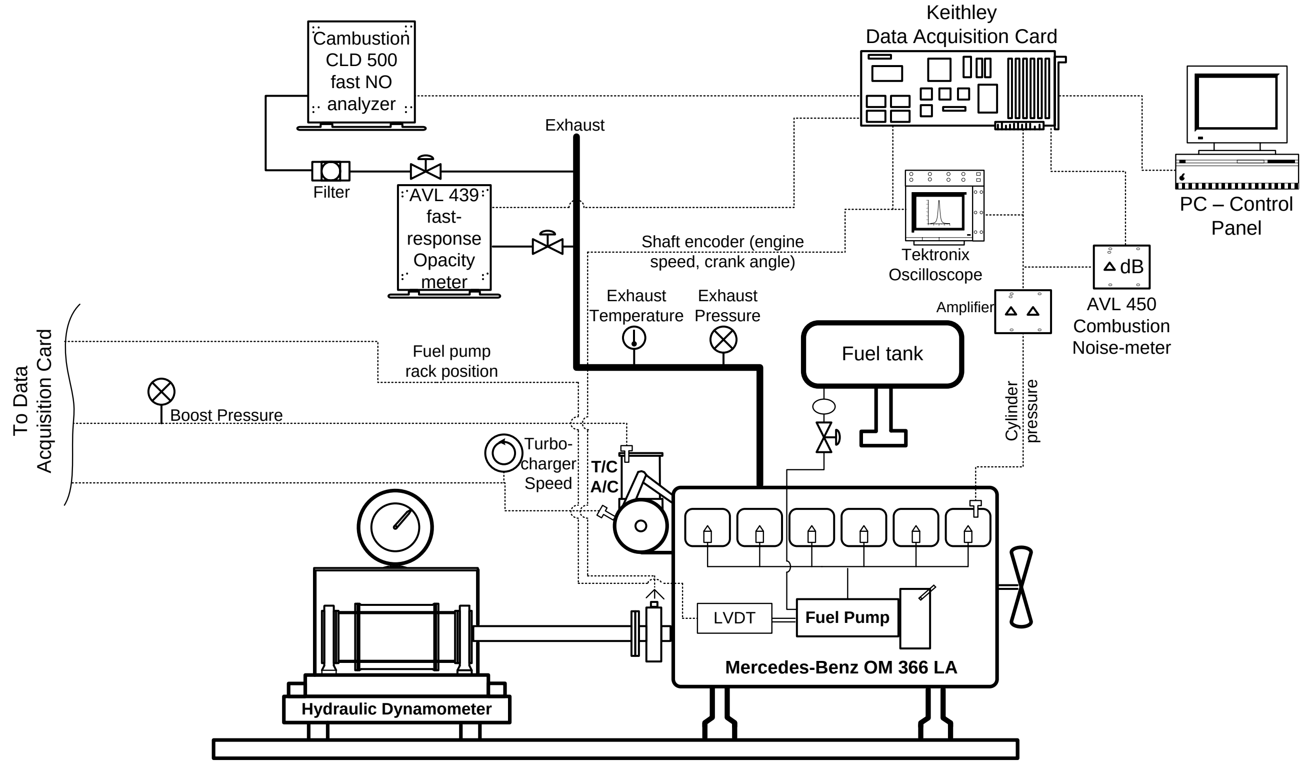

Fig. 1 Rakopoulos et al.

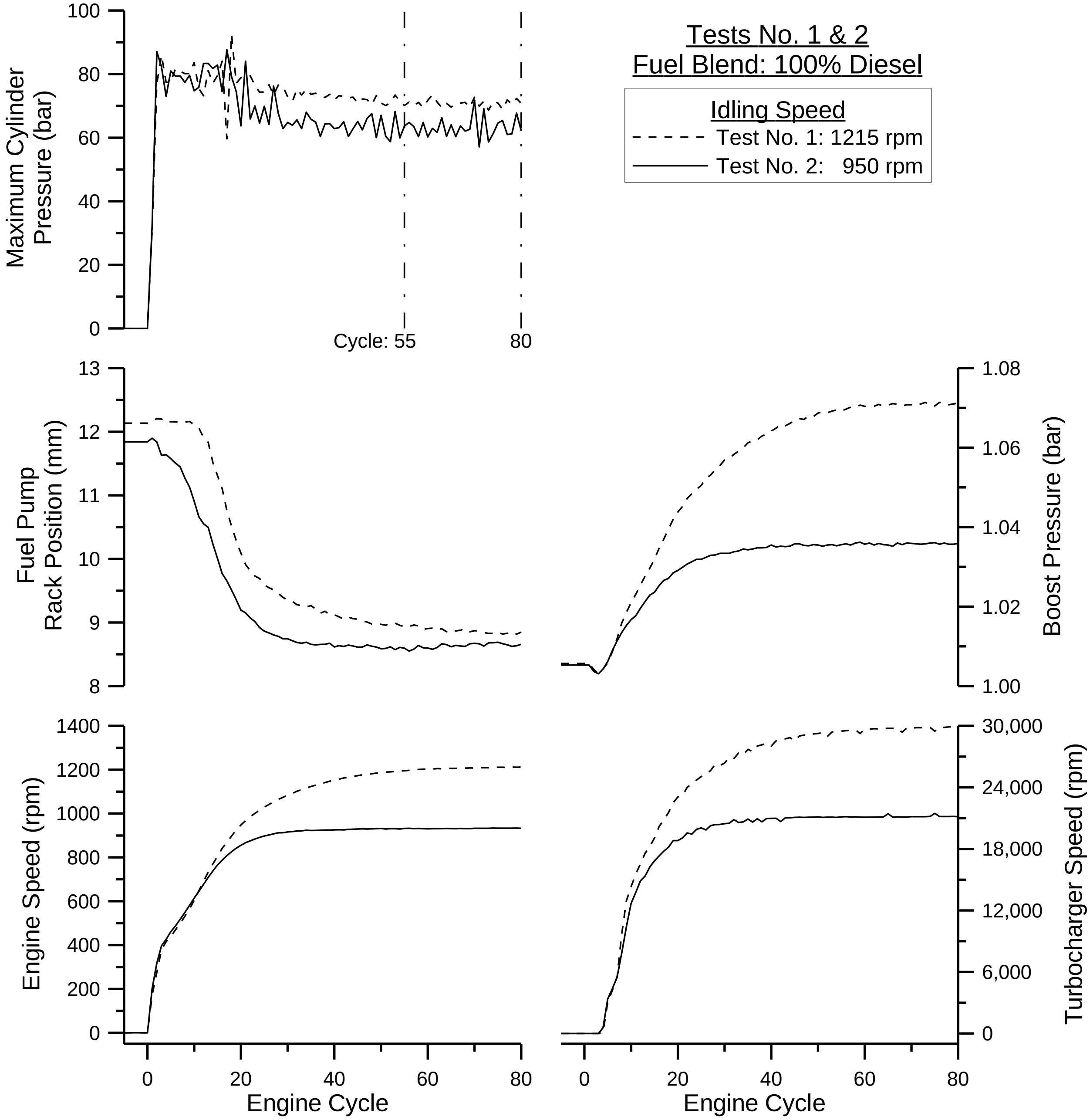

Fig. 2 Rakopoulos et al.

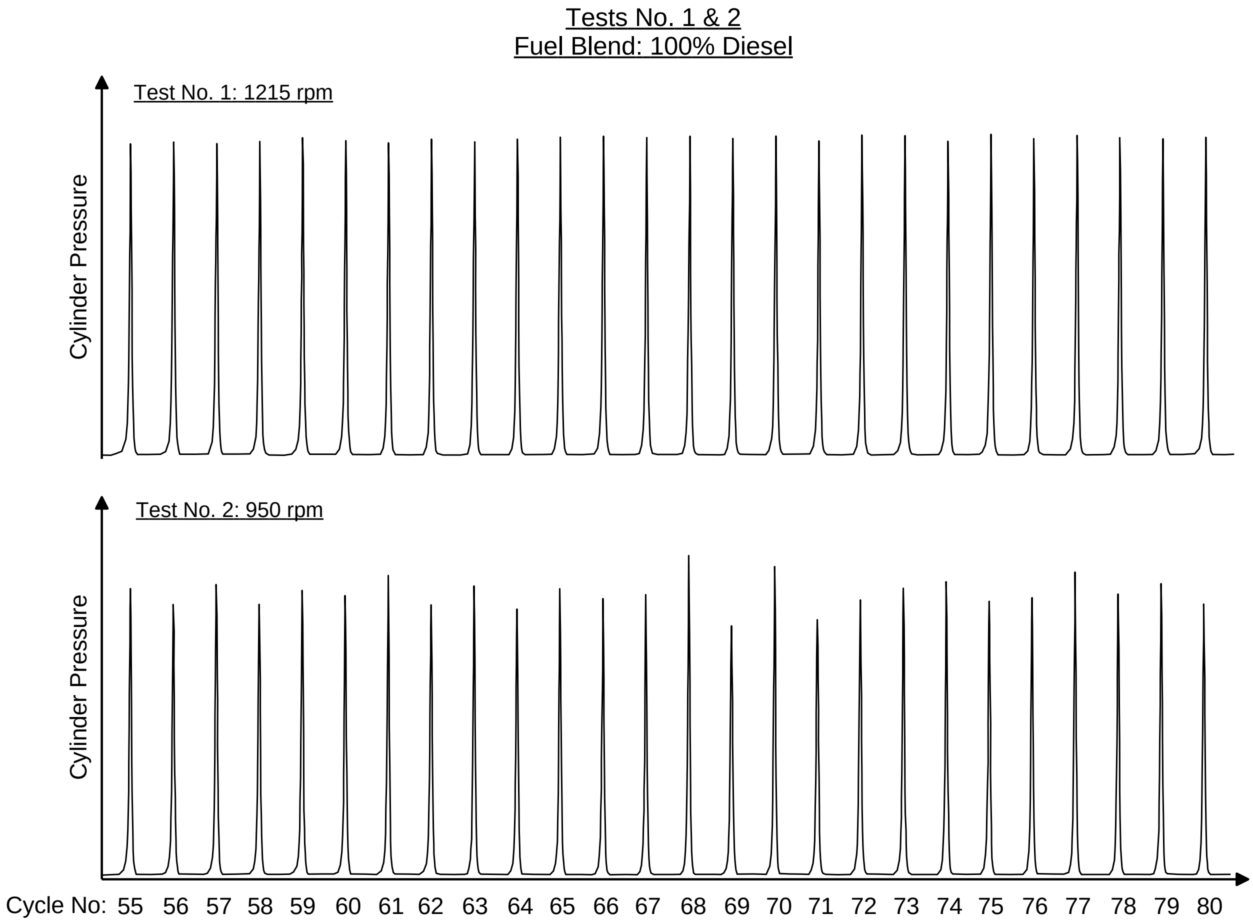

Fig. 3 Rakopoulos et al.

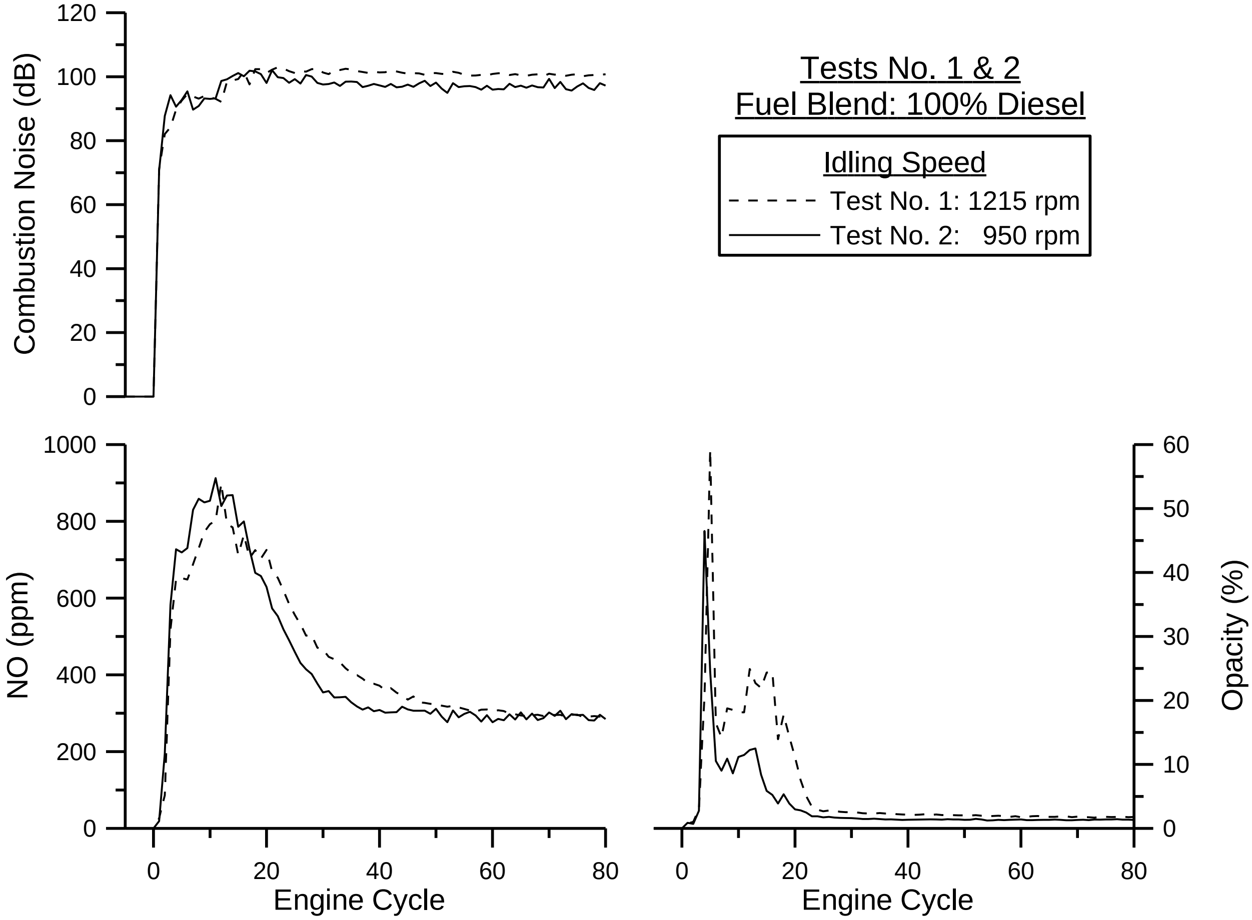

Fig. 4 Rakopoulos et al.

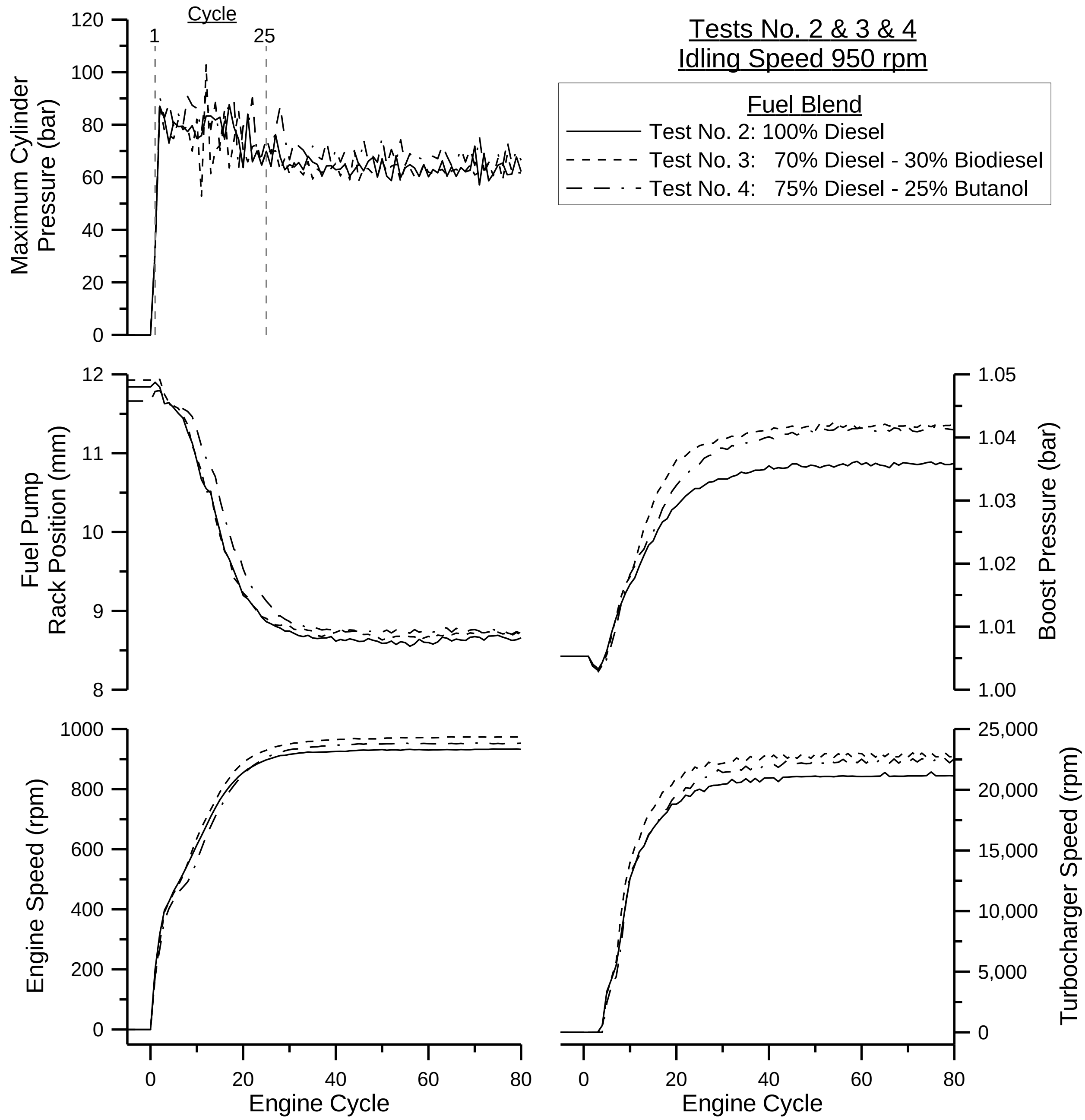

Fig. 5 Rakopoulos et al.

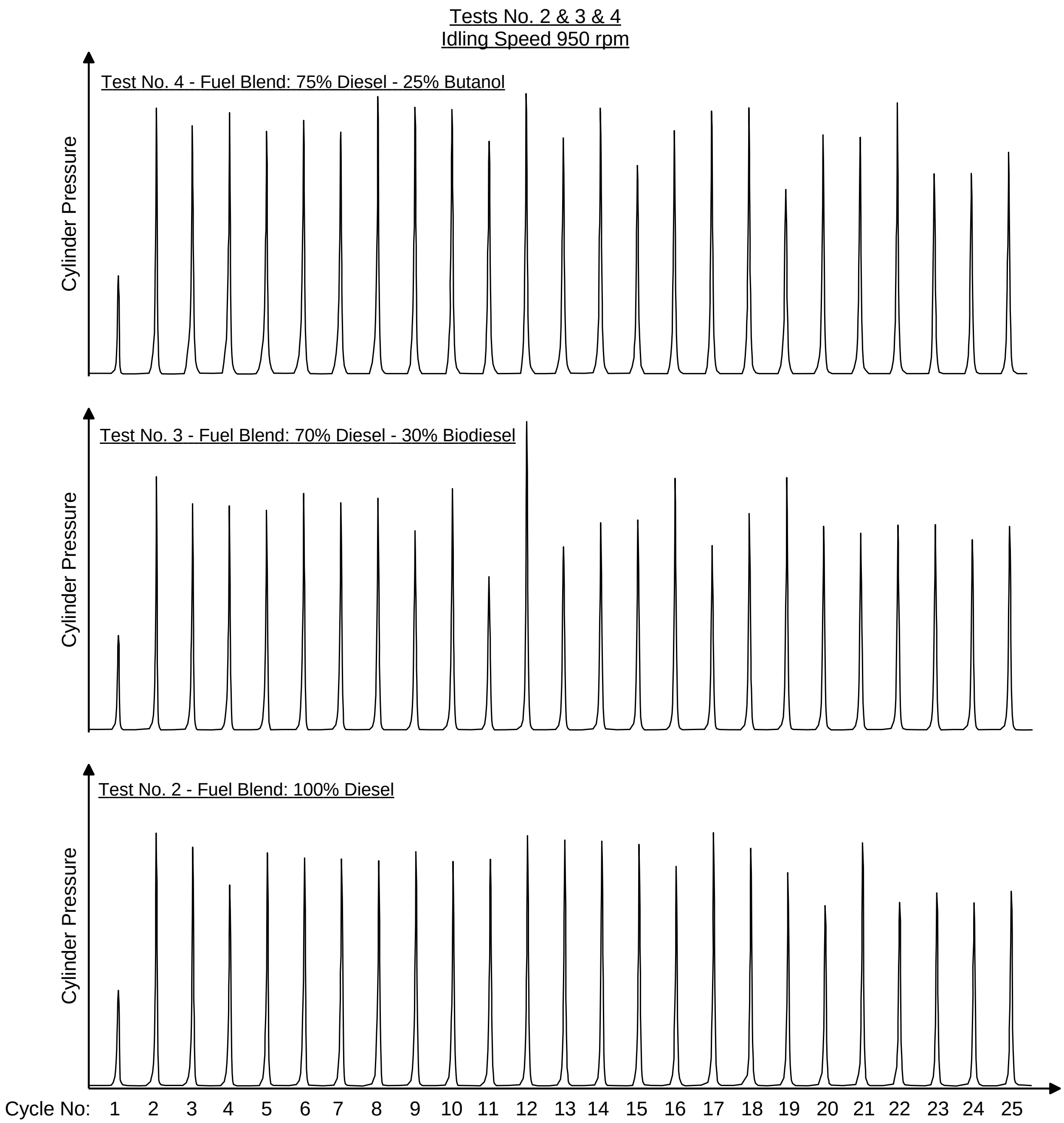

Fig. 6 Rakopoulos et al.

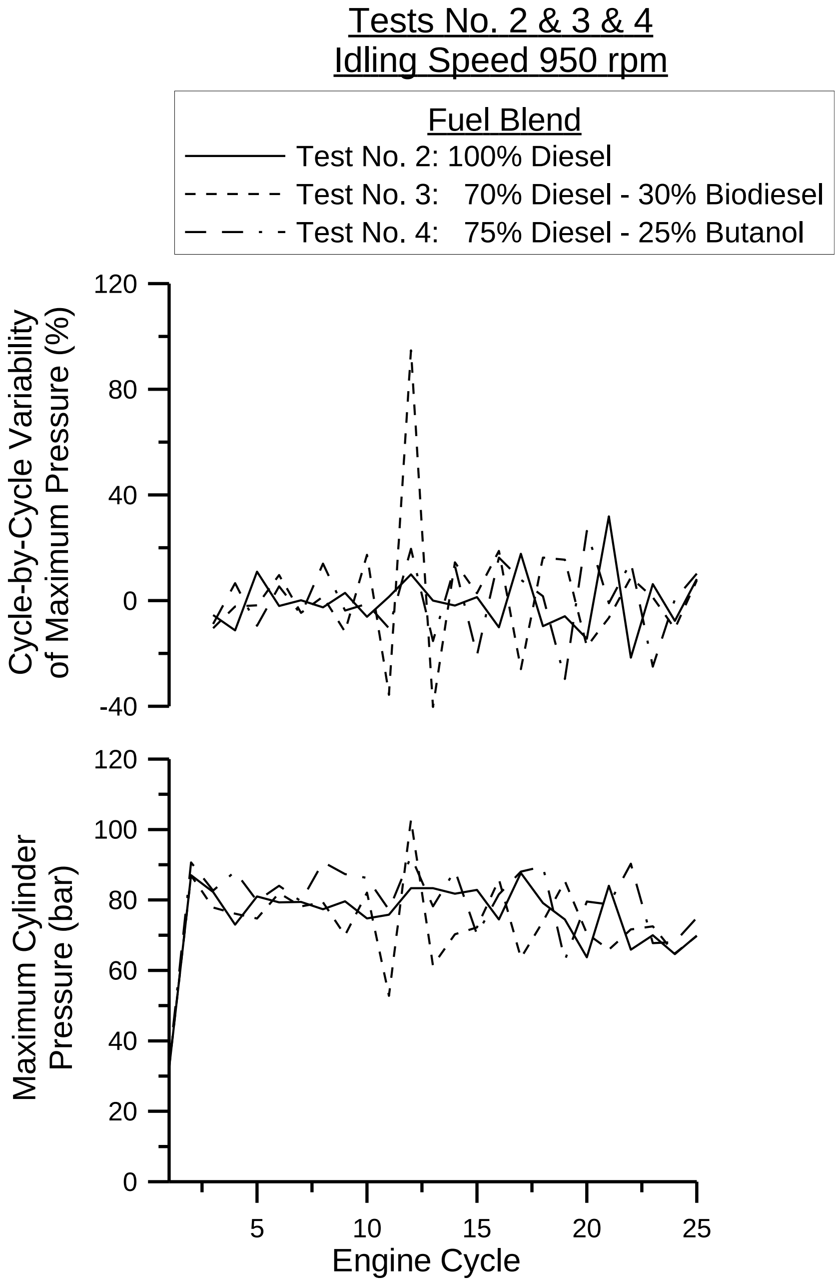

Fig. 7 Rakopoulos et al.

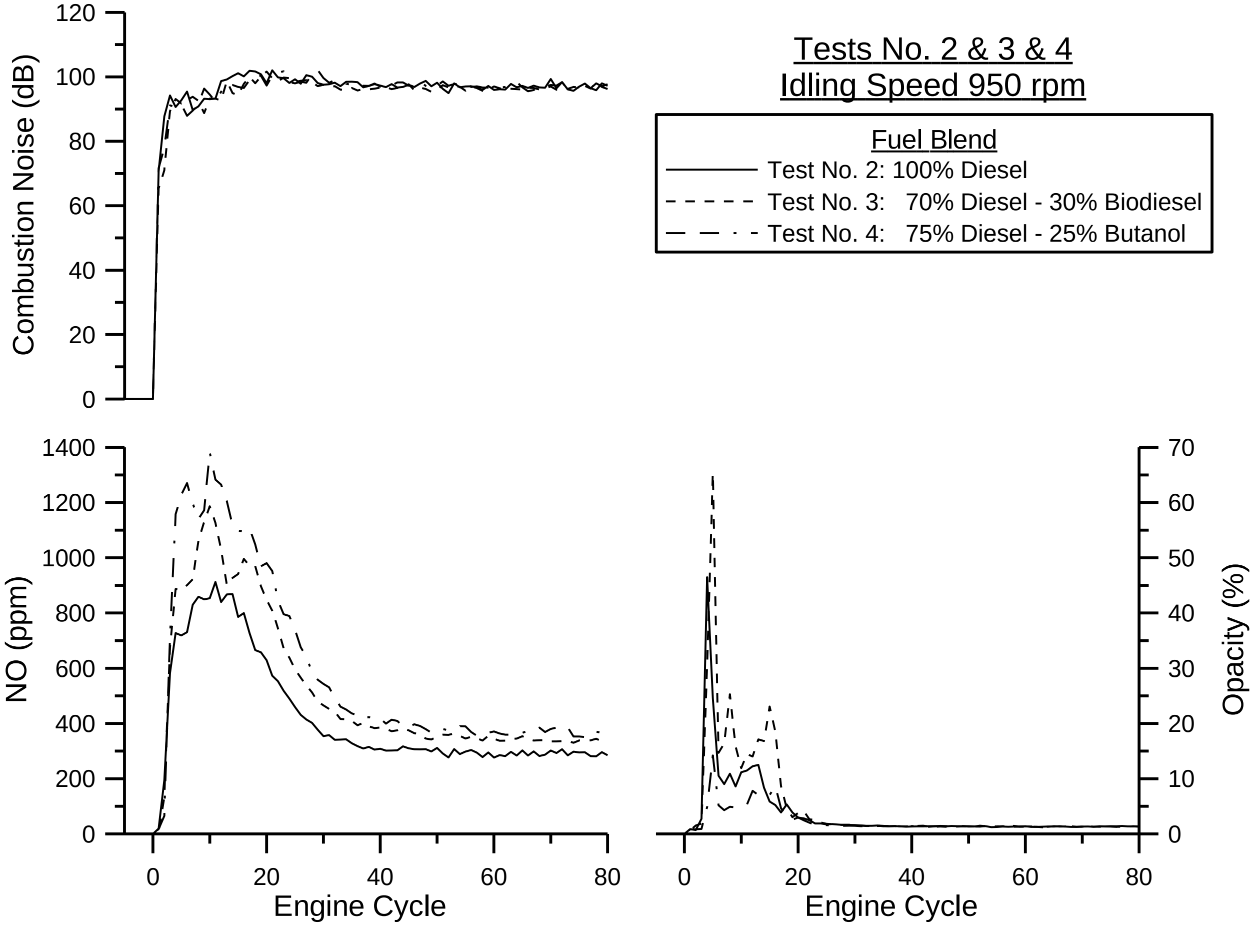

Fig. 8 Rakopoulos et al.